Optics Letters

10 W-level gain-switched all-fiber laser at 2.8 μm

Pascal Paradis,* Vincent Fortin, Yigit Ozan Aydin, Réal Vallée, and Martin Bernier

Centre d'optique, photonique et laser (COPL), Université Laval, Québec, Québec G1V 0A6, Canada
**Corresponding author: pascal.paradis.2@ulaval.ca*

Received 30 April 2018; revised 3 June 2018; accepted 4 June 2018; posted 7 June 2018 (Doc. ID 330672); published 29 June 2018

We report a simply designed gain-switched all-fiber laser emitting a maximum average output power of 11.2 W at 2.826 μm. The corresponding extracted pulse energy is 80 μJ at a pulse duration of 170 ns. These performances significantly surpass previous gain-switched demonstrations and are close to the state-of-the-art *Q*-switched laser performances near 2.8 μm, but with a much simpler and robust all-fiber design. The spliceless laser cavity is made of a heavily erbium-doped fluoride glass fiber and is bounded by fiber Bragg gratings written directly in the gain fiber through the protective polymer coating.

OCIS codes: (140.3510) Lasers, fiber; (140.3538) Lasers, pulsed; (140.3500) Lasers, erbium.

https://doi.org/10.1364/OL.43.003196

High-power CW and pulsed lasers operating near 3 μm have generated considerable interest in recent years due to their proximity to the fundamental absorption of liquid water [1,2]. The high-power emission centered on the peak absorption of water is particularly appealing for biomedical applications [3], particularly in orthopedics [4], dentistry [5], dermatology [6], and ophthalmology [7]. Powerful and bright fiber lasers operating in the vicinity of 3 μm can also be used as a pump to generate efficient supercontinuum covering the 3–5 μm atmosphere transmission window [8], where various ro-vibrational absorption lines of gas pollutants are resonant [9]. Thus, these laser sources are interesting for short and long-range applications such as gas spectroscopy [10–12] and military countermeasures [13]. For field applications, the laser systems must generally be stable, energetically efficient, compact and, more importantly, robust.

Several pulsed lasers near 2.8 μm, be it mode-locked, *Q*-switched, or gain-switched have already been demonstrated [14–18]. Antipov *et al.* recently demonstrated a mode-locked holmium-doped fiber laser with an average power of 327 mW and a peak power of 37 kW (pulse energy of 7.6 nJ) [18]. Tokita *et al.* reported a *Q*-switched erbium-doped fluoride glass fiber laser (EDFL) placed in a nitrogen purged enclosure that extracted 12 W of average power and 0.9 kW of peak power (pulse energy of 100 μJ) [15]. Shen *et al.* recently demonstrated a *Q*-switched EDFL with an average power of 1.5 W and a peak power up to 1.6 kW (pulse energy of 0.15 mJ) at 10 kHz [19]. Gorjan *et al.* reported a gain-switched EDFL with 2 W of average power, 68 W of peak power, and 307 ns of pulse duration at 100 kHz [14]. Wei *et al.* demonstrated the first broadly tunable gain-switched EDFL around 3 μm [20], and Luo *et al.* reported on the first dual-waveband gain-switched fiber laser emitting around 2 and 3 μm [21]. In all these demonstrations, the cavity design involved free space optics (e.g., lenses, acousto-optic modulators [AOMs], saturable absorbers, isolators, and/or wave plates), which poses reliability and scalability issues for field applications. Among the three pulsed mechanisms described above, gain switching is the only one that can benefit from existing mid-IR fiber components to enable high-power operation in an all-fiber design [22], since it uses pump modulation to generate the laser pulses.

In this Letter, a simple monolithic gain-switched EDFL operating at 2.826 μm is presented with output performances competing with state-of-the-art *Q*-switched lasers operating near 2.8 μm. With a maximum average output power of 11.2 W (420 W of peak power), a pulse energy of 80 μJ and a pulse duration of 170 ns, the output performances significantly surpass those of previous gain-switched demonstrations in the same wavelength range. These performances are achieved in a robust monolithic laser cavity bounded by intracore fiber Bragg gratings (FBGs) written directly in the gain fiber through the protective polymer coating. The stable operation of the laser is demonstrated over 20 h of continuous operation at high power.

The experimental setup of the gain-switched all-fiber laser is presented in Fig. 1. The linear cavity is made of a heavily (7%) erbium-doped fluoride fiber *(Le Verre Fluoré)* bounded by two FBGs written using femtosecond pulses and the scanning phase mask technique [23]. Both FBGs are written directly in the

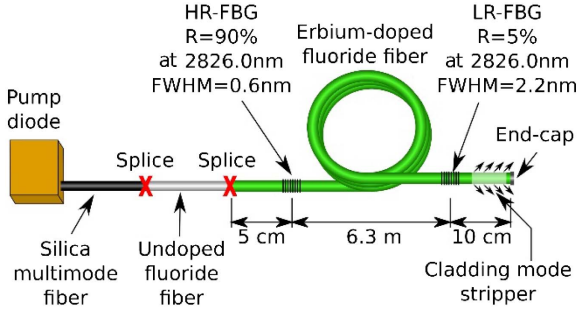

Fig. 1. Schematic diagram of the monolithic gain-switched erbium-doped fluoride fiber laser emitting at 2826 nm.

erbium-doped fiber core through the protective coating to preserve the integrity and the robustness of the pristine fiber [24]. Moreover, this approach lowers the intracavity losses and simplifies the cavity design by avoiding single-mode fluoride fiber splices. Both FBGs have a central wavelength of 2826.0 ± 0.2 nm, whereas their spectral width/reflectivities, respectively, are 0.6 nm/90% for the high reflectivity FBG (HR-FBG) and 2.2 nm/5% for the low reflectivity FBG (LR-FBG). The transmission spectra of the FBGs, along with the laser signal at different output powers, are presented in Fig. 2. Since the laser emission is controlled by the HR-FBG in this laser configuration, a slight spectral shift of the signal towards longer wavelengths is observed when the pump power is increased. This is due to the thermal expansion of the HR-FBG caused by the high pump absorption at the input end of the doped fiber. Accordingly, the LR-FBG was designed with a broad bandwidth (2.2 nm) to ensure a good spectral overlap at different pump/output powers.

The system is pumped with a high-power fiber-coupled 976 nm laser diode (nLight, element e18) emitting up to 220 W with a spectral width of 7 ± 1 nm. Considering the low duty-cycle operation used in the experiment (below 20%), the central peak wavelength of the diode ranges between 965 and 968 nm, depending on the average pump power. The pump diode is modulated using a fast linear modulator (Messtec Power Converter GmbH, VFM 20-50), which was electronically optimized for the diode to provide a high stability of the pump pulses. The modulator is controlled by a digital pulse generator (Stanford Research Systems, SRS, DG-535). The silica glass pump fiber (200 μm core diameter, 0.22 NA) is spliced directly to an undoped double-clad fluoride glass fiber (Le Verre Fluoré) with a cladding diameter of 250 μm and a NA of 0.46. This multimode splice between the fluoride and the silica fibers was achieved with an iridium filament splicer (*Vytran*, GPX-3400) using the approach outlined in Ref. [25]. The undoped fluoride glass fiber is then spliced to the erbium-doped fiber (Le Verre Fluoré), which provides gain for the laser cavity. This active fiber has a core diameter of 15 μm with a NA of 0.12 and is doped at 7 mol.% erbium. Its cladding has a 240 × 260 μm double-*D* shape and is coated with a low-index fluoroacrylate polymer to enable pump guiding. An AlF_3 end cap is spliced to the output end of the doped fiber to prevent long-term degradation from the 2.8 μm laser signal, while providing a single transverse mode output beam [26]. To remove any residual pump at the output, a cladding mode stripper was fabricated by recoating the last 5 cm of active fiber with a high-index polymer. A germanium filter also was placed in front of the power detector to remove any signal below 1.9 μm, thus ensuring that only the 2.8 μm signal was detected.

The average power is measured with a thermopile detector (*Gentec-EO*, UP19K-50F-W5), while the pump and signal spectra are acquired with grating-based optical spectrum analyzers (*Yokogawa*, AQ6373B and AQ6376). The pump and signal temporal profiles, respectively, are measured with a 1 ns rise-time Si detector (*Thorlabs*, FDS010) and a 200 ps rise-time InGaAs detector (*ALPHALAS*, UPD-5N-IR2-P).

Figure 3 presents a typical pulse train for the pump and signal, as well as their respective temporal profile (inset). For the pump, the peak power was calibrated by applying the maximum operating current to the diode. The signal peak power was calculated from the measured waveform and average power. Throughout the experiment, the pump pulse duration was adjusted for each measurement so that it stops just before the signal pulse is emitted. Such synchronization was critical to achieving the highest average and peak powers from the gain-switched laser in this Letter, while preventing the onset of a secondary pulse per cycle. The signal pulses shown in Fig. 3 were obtained at a repetition rate of 140 kHz and had an average output power of 11.2 W. Their averaged peak power was evaluated at 420 W, the highest achieved, with a peak-to-peak variation of 16% over 1 ms. Such a variation mainly results from the formation of substructures in the gain-switched pulse envelope. We believe that these substructures are the result of the mode beating of intracavity longitudinal modes, as reported in previous gain-switched lasers based on Yb-doped and Tm-doped fibers [27,28]. It appears that the substructures are somewhat less stable compared to previous reports [28,29]; we believe this is due to the onset

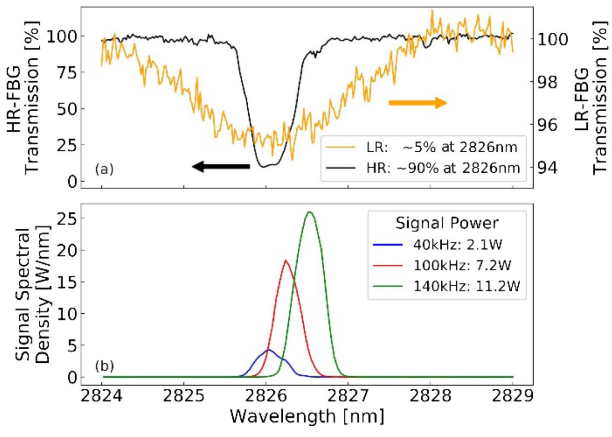

Fig. 2. (a) Transmission spectrum of the FBGs and (b) output laser spectra under different operating conditions (140 kHz, 11.2 W; 100 kHz, 7.24 W; 40 kHz, 2.12 W).

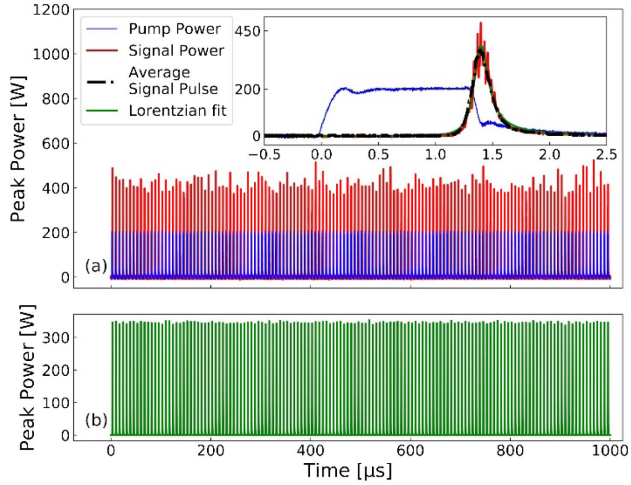

Fig. 3. (a) Typical pulse train at 11.2 W output power and 140 kHz repetition rate. The inset shows an example of timing synchronization of the pump and signal pulses, as well as a signal pulse averaged over 60 samples. The signal peak power is evaluated at 420 ± 70 W. (b) Lorentzian fit for each pulse shows the average gain-switched envelope. The average peak power is 345 W with an RMS variation of 3 W.

of thermo-optic instabilities at high pump and signal power, particularly considering the large number of longitudinal modes in the current long length cavity. Figure 3(b) shows the averaged pulse envelopes obtained with a Lorentzian fit for each pulse; the peak power of the smoothed pulse is found to be 345 W with a root mean-square (RMS) peak-to-peak variation of 3 W (i.e., less than 1%).

As illustrated in Fig. 4, we first investigated the output performances of the cavity at different repetition rates using a constant pump peak power of 210 W, the maximum available from the setup. We can observe from this figure that the FWHM pulse duration of the signal decreases with increasing repetition rates, i.e., from 250 ns (5 kHz) to about 170 ns (140 kHz). Meanwhile, the pulse energy rises from 60 to 80 μJ, and the average output power rises from 75 mW to 11.2 W over the same range of repetition rates. This behavior could be explained by the dynamics of the gain-switched cavity considering a second pulse would build up before the next cycle at a low repetition rate if the pump pulse duration and peak power were the same as at a higher repetition rate. The optical conversion efficiency of the cavity at 140 kHz is about 28% (i.e., 11.2 W average output power for an average pump power of 40.0 W), a value close to typical values reported from similar laser configurations in CW operation [24], i.e., not too far from the Stokes efficiency (34%) of this laser system.

Figure 5 shows the duration, energy, and peak power of the signal pulses with respect to the incident pump pulse energy and duration, at a fixed repetition rate of 100 kHz. The pump pulse duration is optimized in order to maximize the pulse energy in a single pulse regime. With higher pump peak powers, the duration of output pulses decreases, while their energy and average power increase. Based on those results, it appears that the highest possible pump peak power is critical for obtaining the highest signal pulse energy and peak power in such a gain-switched cavity. We believe that a higher pump peak power builds a stronger population inversion (more energy stored in the upper laser level) before the main signal pulse builds up inside the cavity. Then, since the laser gain is higher, the signal pulse power becomes higher and depopulates the upper laser level faster which gives a shorter pulse duration and, consequently, a higher signal peak power [30]. Considering the results obtained in Figs. 4 and 5, the best output performances (i.e., shortest durations, highest energies, and average powers) are obtained for higher pump peak powers at higher repetition rates.

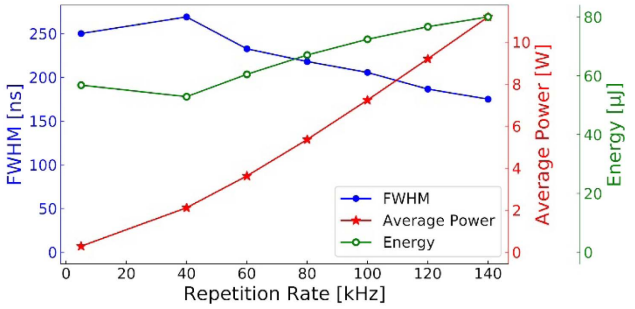

Fig. 4. Repetition rate effect on the pulse duration (FWHM), energy, and average output power. The pump peak power was set at 210 W.

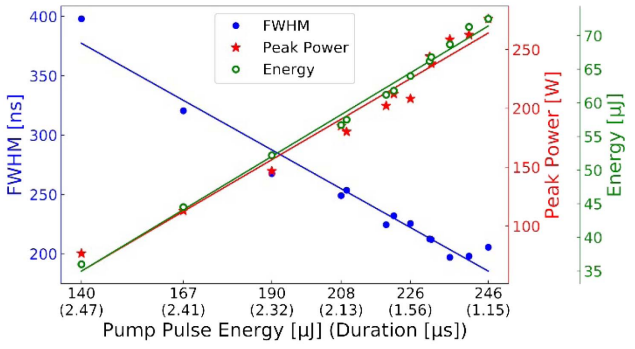

Fig. 5. Energy, duration, and peak power of the signal pulses as a function of the pump pulse energy and duration, for a fixed repetition rate of 100 kHz. For each point, the pump peak power and duration are adjusted to prevent the onset of a secondary pulse per cycle.

The output power stability of the laser system was assessed over a 20 h continuous test, as shown in Fig. 6. The laser showed a long-term output power fluctuation from 7.00 to 7.10 W (100 kHz), with a maximum RMS variation of 0.2% over 1 h. We believe that this small variation can be explained by slight changes in the system temperature, since both the power efficiency and the central wavelength of the pump diode (consequently, the absorbed pump power) are affected by the temperature.

It should be noted that the laser performances reported here are limited by a few factors. The main limitation is the available pump peak power of 210 W. This number could be significantly increased by using an array of synchronized diodes or a pulsed fiber laser at 980 nm [31], which could result in a significant increase of the signal peak power and a decrease of the pulse duration. Numerical modeling of this gain-switched laser is ongoing to further improve the understanding of the dynamics of the system and optimize its design (e.g., fiber length, FBG reflectivity). Another limitation for increasing the average output power is the temperature at the pump input end of the heavily erbium-doped fiber. During the experiment, the repetition rate was limited to 140 kHz to prevent the temperature of the erbium-doped fiber at the pump end from

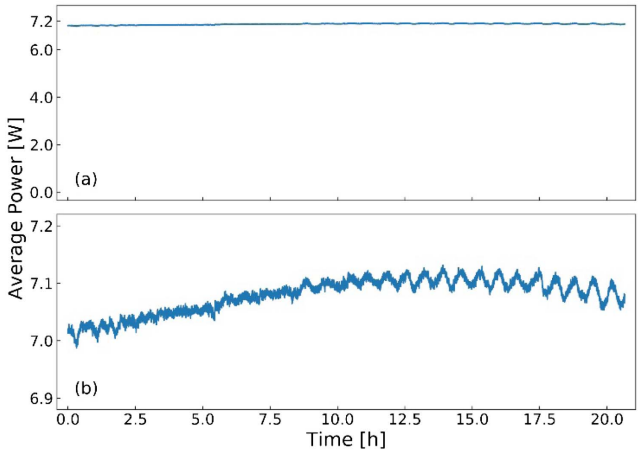

Fig. 6. (a) Laser output power over a period of 20 h. A slight long-term variation of less than 1% of the 7.05 W average power is observed. (b) shows a zoomed view of (a).

exceeding 90°C. With a better heat dissipating setup or an optimized fiber design, the repetition rate could be further increased, thus increasing the average output power [22]. In addition, according to the present results, the pulse duration should also decrease, and the peak power should increase.

In the near future, the amplification of the output pulses will be investigated to achieve pulse energies of a few hundred microjoules to enable biomedical applications, particularly for hard tissue cutting, which requires high pulse energies to be efficient [32]. Eventually, high-power supercontinuum generation might also be possible from this amplified source, provided the peak power of the amplified signal is high enough to trigger nonlinear effects in the fiber [8].

To summarize, a monolithic gain-switched EDFL emitting a maximum average output power of 11.2 W with pulse energies up to 80 μJ and a pulse duration as short as 170 ns is demonstrated. The 7.05 W average output power fluctuates by less than 1% over 20 h of continuous operation. These results represent a significant improvement over the previous state-of-the-art gain-switched EDFL from Gorjan *et al.* [14] and are close to those of the nitrogen purged *Q*-switched laser from Tokita *et al.* [15] with a much simpler design. An average efficiency of 28% is obtained, which could be further increased by optimizing the cavity design. A better thermal management of the doped fiber should enable operation at higher repetition rates with higher average output powers. A pump source with higher peak power should also enable the generation of significantly higher peak power pulses with shorter duration. This demonstration is a step towards field applications of pulsed high-power erbium-doped fiber lasers emitting around 3 μm.

Funding. Natural Sciences and Engineering Research Council of Canada (NSERC) (CG101779, CG112389); Canada Foundation for Innovation (CFI) (GF072345); Fonds de Recherche du Québec—Nature et Technologies (FRQNT) (CO201310, FT097991).

Acknowledgment. The authors thank Frédéric Jobin and Frédéric Maes for their help with the end cap and the silica to fluoride glass fiber splice. The authors also thank Simon Duval for fruitful discussions on pulsed lasers.

REFERENCES

1. X. Zhu, G. Zhu, C. Wei, L. V. Kotov, J. Wang, M. Tong, R. A. Norwood, and N. Peyghambarian, J. Opt. Soc. Am. B **34**, A15 (2017).
2. S. D. Jackson, Nat. Photonics **6**, 423 (2012).
3. S. D. Jackson and A. Lauto, Lasers Surg. Med. **30**, 184 (2002).
4. S. Stübinger, Clin. Cosmet. Invest. Dent. **2**, 47 (2010).
5. J. Diaci and B. Gaspirc, J. Laser Health Acad. **1**, 1 (2012).
6. J. D. Holcomb, Facial Plast. Surg. Clin. North Am. **19**, 261 (2011).
7. T. Klink, G. Schlunck, W. E. Lieb, J. Klink, and F. Grehn, Eye **22**, 370 (2008).
8. J.-C. Gauthier, V. Fortin, S. Duval, R. Vallée, and M. Bernier, Opt. Lett. **40**, 5247 (2015).
9. J. Swiderski, M. Michalska, and G. Maze, Opt. Express **21**, 7851 (2013).
10. R. N. Clark and T. L. Roush, J. Geophys. Res. [Solid Earth] **89**, 6329 (1984).
11. S. Lambert-Girard, M. Allard, M. Piché, and F. Babin, Appl. Opt. **54**, 1647 (2015).
12. F. K. Tittel, D. Richter, and A. Fried, in *Solid-State Mid-Infrared Laser Sources* (Springer, 2003), pp. 458–529.
13. H. H. P. T. Bekman, J. C. van den Heuvel, F. J. M. van Putten, and R. Schleijpen, Proc. SPIE **5615**, 27 (2004).
14. M. Gorjan, R. Petkovšek, M. Marinček, and M. Čopič, Opt. Lett. **36**, 1923 (2011).
15. S. Tokita, M. Murakami, S. Shimizu, M. Hashida, and S. Sakabe, Opt. Lett. **36**, 2812 (2011).
16. H. Luo, J. Li, J. Xie, B. Zhai, C. Wei, and Y. Liu, Opt. Express **24**, 29022 (2016).
17. H. Luo, J. Li, Y. Hai, X. Lai, and Y. Liu, Opt. Express **26**, 63 (2018).
18. S. Antipov, D. D. Hudson, A. Fuerbach, and S. D. Jackson, Optica **3**, 1373 (2016).
19. Y. Shen, Y. Wang, K. Luan, H. Chen, M. Tao, and J. Si, Appl. Phys. B **123**, 105 (2017).
20. C. Wei, H. Luo, H. Shi, Y. Lyu, H. Zhang, and Y. Liu, Opt. Express **25**, 8816 (2017).
21. H. Luo, J. Li, C. Zhu, X. Lai, Y. Hai, and Y. Liu, Sci. Rep. **7**, 16891 (2017).
22. V. Fortin, M. Bernier, S. T. Bah, and R. Vallée, Opt. Lett. **40**, 2882 (2015).
23. M. Bernier, D. Faucher, R. Vallée, A. Saliminia, G. Androz, Y. Sheng, and S. L. Chin, Opt. Lett. **32**, 454 (2007).
24. M. Bernier, F. Trépanier, J. Carrier, and R. Vallée, Opt. Lett. **39**, 3646 (2014).
25. K. Yin, B. Zhang, J. Yao, L. Yang, S. Chen, and J. Hou, Opt. Lett. **41**, 946 (2016).
26. N. Caron, M. Bernier, D. Faucher, and R. Vallée, Opt. Express **20**, 22188 (2012).
27. C. Larsen, K. P. Hansen, K. E. Mattsson, and O. Bang, Opt. Express **22**, 1490 (2014).
28. J. Swiderski and M. Michalska, Opt. Lett. **38**, 1624 (2013).
29. P. Paradis, V. Fortin, Y. O. Aydin, F. Jobin, S. Duval, R. Vallée, and M. Bernier, in *Optics InfoBase Conference Papers* (2017), Vol. **Part F75-A**.
30. M. Jiang and P. Tayebati, Opt. Lett. **32**, 1797 (2007).
31. J. Boullet, R. Dubrasquet, C. Médina, R. Bello-Doua, N. Traynor, and E. Cormier, Opt. Lett. **35**, 1650 (2010).
32. P. Spencer, J. M. Payne, C. M. Cobb, L. Reinisch, G. M. Peavy, D. D. Drummer, D. L. Suchman, and J. R. Swafford, J. Periodontol. **70**, 68 (1999).